CHEMISTRY
A European Journal

A Journal of
ChemPubSoc Europe

Accepted Article

Title: Synthesis of AgWCNx nanocomposite for one-step conversion of Cyclohexene to Adipic Acid and its mechanistic studies

Authors: Reena Goyal, Sidarth Sameer, Arijit Bag, Bipul Sarkar, Nikita Singhal, and Ankur Bordoloi

To be cited as: *Chem. Eur. J.* 10.1002/chem.201703111

Link to VoR: http://dx.doi.org/10.1002/chem.201703111

Supported by
ACES

WILEY-VCH

10.1002/chem.201703111

WILEY-VCH

FULL PAPER

Synthesis of AgWCNx nanocomposite for one-step conversion of Cyclohexene to Adipic Acid and its mechanistic studies

Reena Goyal,[a] Siddharth Sameer, [a] Bipul Sarkar, [a,b] Arijit Bag, [c] Nikita Singhal, [a] and Ankur Bordoloi*[a]

Novel silver nanoparticles grafted on W-CNx catalyst has been prepared by using a facile pH adjusted method. The material reported a non-mineral acid route for the synthesis of industrially significant monomers adipic acid (*aa*), via selective oxidation of cyclohexene. Ag has been stabilized into the hydrophobic matrix during the formation of mesoporous silica material using aniline as a stabilizing agent. A cyclohexene conversion of 92.2% with 96.2% *aa* selectivity was observed with AgWCNx-2 catalyst; were AgWCNx catalyst found efficient for the direct conversion of adipic acid in respect to their monometallic counters. The energy profile diagram for each reaction path of AgWCNx catalyst were studied along with their monometallic counters using Gaussian 09 package. The reported material can avoid the use of harmful phase transfer catalyst (PTC) and/or chlorinated additives are among the other benefits of the reported work.

Introduction

The concept of metals nanoparticles supported on carbon materials has gained much attention. Although, the homogeneous immobilization of different transition metal nanoparticles on mesoporous CNx materials not only favors metal support interaction but also enhance the capability of catalyst for industrial application.[1] In our previous report, we have shown the importance of immobilization of WOx nanoclusters on MCNx for acid-base co-operative catalysis.[2] Such transition metal supported nitrogen enriched carbon material are usually synthesized by various chemical process including pyrolysis hydrothermal and polymerization. Different technique to stabilize metal nanoparticles on MCNx framework is also been reported earlier. Although, to the best of our knowledge no effort has been made on in-situ synthesis of bimetallic nanoparticles on mesoporous carbon nitride material. In particular the bimetallic nanoparticles on high porosity nitrogen enrich carbon material if been synthesized it would be of great significance. Remarkable catalytic efficiency of silver nanoparticles on WO_3 oxide support has already been reported by Bal *et.al*.[3] with regards to the role of silver nanoparticles and WO_x in cyclohexene oxidation they have experienced the synergy effect between small size of silver nanoparticles and tungsten oxide species. Moreover, the dispersion of silver tungsten oxide nanoparticles on high surface area material will further enhance the accessibility of active sites towards reactant. As part of our ongoing effort, silver tungsten oxide nanoparticles supported mesoporous nitrogen enrich carbon material has been synthesized and being employed for the selective oxidation of cyclohexene to adipic acid. It was observed that adipic acid (*aa*) from cyclohexene can outline a high flexible and versatility eco-friendly *aa* production process.

Adipic acid is the largest building block for the synthetic fibers industry.[4] It is used for the manufacturing of nylon 6, 6, plasticizers, adiponitriles, tire reinforcements, plastics, urethane foams, elastomers, low temperature synthetic lubricants etc.[5] With the ever increasing demand (3.5 million tons per annum) and persistent environmental issues associated with current commercial (Dupont and Asahei kasei process) adipic acid production process demands for a new alternative. Owing to these factors several environmental benign protocol has been designed and investigated such as oxidative cleavage of 1,2-diol by HNO_3[5a] and oxidation of 1,2-diol or cycloalkanones [6] by hydrogen peroxide. Therefore, in the search of developing a less polluting and greener routes, direct synthesis of cyclohexene to adipic acid is most relevant approach from the industrial point of view.[7] Moreover, the use of cyclohexene is a viable substrate as its availability is continuously increasing with hydrogenation of benzene [8] or dehydrogenation of cyclohexane [9] in the last several years. The groundbreaking work has been done by Sato *et. al*., as they reported a phase transfer catalyst $[CH_3(n\text{-}C_8H_{17})N]HSO_4$ for direct oxidation of cyclohexene with H_2O_2.[5b] This eco-friendly, non–nitric acid route find difficulties because of the production cost of H_2O_2 along with the separation of homogeneous catalyst from product steams. Nevertheless, the negative environmental impact of quaternary ammonium ions noticed by Deng *et. al*. has forced to withdraw its commercial usages.[10] After this work various tungsten based catalyst system has been reported like $[BMIm]_2\ WO_4$ supported on silica sulphamic acid,[11] $[WO(O_2)_2.2QOH]$,[12] $H_3PW_{12}O_{40}$,[13] and combinations of Na_2WO_4 with H_2SO_4[14] or H_2WO_4 in H_2O_2 medium. However, all the above reported catalyst suffer from environmental issues and separation problem. The TAPO-5[15] and titanium grafted Al/SBA-15[8c, 16] is also been reported for direct conversion of cyclohexene to adipic acid with TBHP (*tert*-butyl hydroperoxide) as oxidizing agent. Despite the high yield

[a] R. Goyal, S. Sameer, N. Singhal, Dr. B. Sarkar, Dr. A. Bordoloi, Nano Catalysis area, Refinery Technology Division, CSIR-Indian Institute of Petroleum, Dehradun-248005, India
E-mail: ankurb@iip.res.in
Tel.: +91 135 2525898; Fax: +91 135 2660202
[b] Dr. Bipul Sarkar
Chemical Science Division, CSIR-Indian Institute of Petroleum, Dehradun-248005, India
[c] Dr. A. Bag
Department of Chemical Sciences, Indian Institute of Science Education and Research Kolkata, West-Bengal, India

Supporting information for this article is given via a link at the end of the document.((Please delete this text if not appropriate))

obtained using titanium based catalyst, the environmental limitation of organic peroxide TBHP as compare to H_2O_2 limits its usage. H_2O_2 is a greener and cheap oxidant with an atomic oxygen efficiency of 47%.[17] H_2O_2 has the efficient potential for the oxidation of cyclohexene to adipic acid in the presence of metal oxide catalyst. Till date, no catalyst system is reported which can produce adipic acid from cyclohexene industrially using H_2O_2 as oxidant. In this context, developing an easily recycled, highly efficient and stable with extensive applicability is appropriate. Within this category metal nanoparticle supported over nitrogen doped carbon material has already been proven as efficient oxidation reduction catalyst.

Results and Discussion

Figure 1a shows the small angle X-ray scattering pattern of the mesoporous carbon materials with different ratio of silver and tungsten. All the samples shows a sharp peak at low angle with two higher order peak which can be assigned to (100), (110) and (200) plane of hexagonal space group *p6mm*.[1-2, 18] The intensity of the peaks are less compared to hard template AgW-SiO_2 (Figure S1, in supporting information). This is probably due to the decrease in number of pores in carbon materials compare to SiO_2. However the unit cell constant parameter calculated from the formula $a_0=2d_{100}/\sqrt{3}$ shows a very slight increase in value with increasing the amount of silver and tungsten. While a common wide angle reflection (Figure 1a, inset) in the region of 25° could be attributed to the reflection from (200) plane of carbon and broadening in peak is due to amorphous nature of materials.[18] Although, the wide angle XRD pattern shows no peak that can be attributed to tungsten oxide. This might be due to the ultra-small particle of WO_3 which is too small to be detected;[19] also indicating well dispersed WO_3 particles on CNx.[20] Otherwise the WO_3 particle were successfully incorporated into the hexagonal channels of CNx material where their size is too little to be completely detected by XRD.[21] Whereas, a very strong diffraction peak at 38.1° corresponding to the face centered cubic (FCC) silver (111) phase (JCPDS no. 4-0787) was observed in different AgWCNx and AgCNx (Figure S2, supporting information) catalysts. A number of strong Bragg reflections was also noticed for higher silver loaded catalyst (e.g. AgWCNx-2 and 3) which correspond to the (200), (220), and (311) reflections of cubic silver. However, XRD does not reveal the presence of WOx peak, while the Raman bands in the range between 200 and 1000 cm^{-1} (Figure 1c and 1d) correspond to the v(W–O–W) stretching mode of WO_3 of AgWCNx materials. It is clear that each of the Raman spectra has four well-resolved peaks between 246-397 and 664-837 cm^{-1}. Peaks centered between 664 and 837 cm^{-1} are attributed to W-O-W stretching vibration mode, whereas the two lower peaks at 246 and 397 cm^{-1} contributed to W-O-W bending mode vibration [(O-W-O)].[22] Increase in tungsten loading shows enhanced Raman intensity by only ~7-8%. However, shift of Raman band with the increase in metal loading suggest due to the presence of isolated double bonds separated by functional groups on the CNx network.[23] For, comparison Raman spectra of parent Ag-W-SiO_2 was given in Figure S3, in supporting information. The Raman spectra for AgWCNx catalyst (Figure 1c) also shows two common Raman band at 1350 and 1580 cm^{-1} that is related to D and G band of carbon material.[24] The appearance of D band is due to the A1g breathing mode from carbon while the G peaks is due to the in plane stretching between sp^2 carbon atoms.

The surface composition of AgWCNx catalyst studied by X-Ray photoelectron spectroscopy also evidenced the presence of WOx and also facts the interaction between Ag and W atoms of catalyst. Figure 2 shows the XPS spectra of W $4f_{7/2}$ and Ag $3d_{5/2}$. The peak at binding energy 35.6 eV (Figure 2b) and 368.3 eV (Figure 2a) in AgWCNx-1 corresponds to the presence of WO_3 and metallic silver within the catalyst. Whereas, a positive shift in binding energy of Ag and negative shift in WO_3 as compare to pure AgCNx and WCNx (Figure S4, supporting information) corresponds to the transfer of electron density from WO_3 to silver atoms.[25] However, the shift in binding energy (BE) is low in higher loading catalyst; this represent the weak interaction between Ag and W within the catalyst. Whereas, the enhancement in relative intensity of peaks with increasing in metal loading is assumed to be because of increase in surface composition of metals. The C 1s spectra of AgWCNx-1 catalyst can be further deconvoluted into five peaks (Figure 2c). The peaks at 284.5 and 285.4 eV binding energy (BE) corresponds to sp^3 hybridized graphite-like carbon and sp^2 hybridized diamond-like carbon.[18, 26] While, the other two peaks at 286.5 and 288.5 eV indicates the presence of oxygen functionalities in the surface such as CO, C=O. The N 1s was also deconvoluted into three peaks, the peaks at 398.9, 400.1, and 403.5 eV are related to the presence of N-pyridine, N-pyrolic, and N-quaternary structure of the AgWCNx-1 catalyst.[1-2, 18]

The field-emission scanning electron microscopy (FESEM) image (Figure 3) clearly reveals the rod shaped morphology.[2] The lateral size of the AgWCNx-2 materials is in the range of 100–200 nm, and obvious waves and corrugations can be observed. A corresponding transmission electron microscopy (TEM) image (Figure 4) shows the rod like fibrous morphology of the AgWCNx materials. The high-resolution transmission electron microscopy (HRTEM) images (Figure 4b-d and S5) shows 0.2-0.3 nm 2D channels, which is consistent with mesopores of 3 to 4 nm this result seems well in agreement with the BJH pore volume detailed in Figure 4d. The fibrous like morphology is more irregular with the increment of silver and tungstate (Figure 4e-f). It seems like a thin layer of amorphous carbon was deposited on the channels of AgWCNx-3 catalyst. The elemental mapping (Figure 2 and S6, supporting information) shows quite homogeneous distribution of Ag and WO_3 on the CNx matrix.

The porosity and surface properties of synthesized materials were examined by N_2 adsorption isotherm Figure 5. The N_2 adsorption isotherm for SBA-15 materials is type IV with H1 hysteresis loop characteristics of mesoporous material (Figure S7, supporting information). However a relative shoulder in the lower pressure region with type II indicating the coexistence of micro and mesopore in the newly synthesized material. It is assumed that structural shrinkage of CNx material during carbonization leads to the formation of micropore in carbon material. NL-DFT confirms the bimodal pore system composed of micropore and mesopore in the material. The BJH isotherm of WCNx exhibit narrow pore size distribution centered at 4.2 nm while the Ag/W/CNx has the bimodal pore with large size mesopores in high loading catalyst. The specific surface area of the materials varies between 349-331 m^2/g with total pore volume between 0.43-0.28 cm^3; where the major contribution comes from mesopores. The steep

capillary condensation in partial pressure 0.45- 0.90 implied the narrow pore size distribution with uniformity in mesoporosity. The surface area of material is appears to systematically decrease with enhancement in the loading of Ag and W metal. This may be due to the blockage of more number of pore by metal nanoparticle on increasing amount of metal.

The H_2 TPR profile of AgCNx (in Figure S8) shows no reduction peak for Ag, as it already in metallic form (as discussed in XPS); whereas the widespan hump can be due to the reduction of N functionality of the CNx. The reduction temperature of WO_3 species can be locate at 467°C for WCNx. The reduction peak for W species for AgWCNx-1, appears at lower temperature in compare to WCNx. While with increase in Ag to W ratio the T_{max} appears to take a positive shift in respect to AgWCNx. This can be due to the increase in particle size upon loading of Ag and W.

Surface Acidity of AgWCNx

The results of NH_3-TPD are briefed in Table 1, whereas the NH_3-TPD profiles are shown in Figure S8. WCNx shows a long span peak for ammonia desorption well above 240°C, signifying the presence of medium and strong acid sites in the material. This NH_3-TPD profiles is in agreement with previous reports for W based material.[27] In contrast, it can be seen that all the AgWCNx material shows desorption peaks at approximately 125–300°C; lower temperature compare to WCNx. Comparing the amount of acid sites, AgWCNx material displays lower amount of acid sites per surface area of the catalyst (Table 1). This can be because of lower loading in case of AgWCNx-1, while for others the W-N or W-Ag weak interaction may significantly decrease the number of acid sites.

Lapisardi *et al*. elaborated the role of acidity on the catalytic activity of bifunctional Ti-AlSBA-15 materials.[16a] In this regard, it is also been found that a high Brønsted acid site increase the rate of acid-catalyzed epoxide opening during the oxidation of cyclohexene to *aa* over zeolite occluded manganese di-imine complexes.[28] We experienced, a sufficient amount of soft acidic site is crucial for *aa* production (Figure S9). We have performed pyridine-IR experiments, however the result was not found satisfactory.

Catalytic activity

The activity of AgWCNx material has been investigated and the result are summarized in Table 2. The reaction rates are shown as TOF and measured in units of moles of adipic acid produced using per mole of silver and tungsten. In absence of catalyst, some oxidation is observed, this is negligible and less selective which confirms the demand of catalyst. Mesoporous CNx also shows similar activity (Table 2, entry 2), those result suggest autocatalysis by H_2O_2 at the reaction temperature. To clearly exploit the catalytic role of individual role of WO_3 and Ag; a series of cyclohexene oxidation experiment on individual metal supported on CNx (Table 2, entry 3-4) is conducted. It is been experienced that cyclohexene oxidation catalyzed by WCNx reaches up to 65.7%; cyclohexane oxide (73.1%) was obtain as the major product along with cyclohexenol, cyclohexenone and other further oxidized product. While the catalyst with Ag loading e. g. Ag-CNx exhibited better oxidation activity (Table 2, entry 4) with very negligible formation of adipic acid. Catalyst prepared by physical mixing (Table 2, entry 5,6) shows low catalytic activity compare to entry 5 and 6. This result clearly suggest, WCNx is a better epoxidation catalyst whereas AgCNx is more on oxidation activity. When we combine both of the metal functionality in CNx matrix the catalyst show extraordinary oxidation property (Table 2, entry 8-10) compare to their monometallic counter.

As can be seen from Table 2, AgWCNx exhibit the highest reaction rate (TOF) when compare to their monometallic counters or impregnated catalyst. AgWCNx-1 gives almost 89.9% cyclohexane conversion with 94.1% adipic acid selectivity. Although, intermediate compound like oxepane-2,7-diol, oxepane-2,7-dione still exist in the reaction medium; this is probably because of insufficient active site for catalysis. When we increased the silver and tungusten loading on CNx (Table 2, entry 9), we noticed complete oxidation of intermediate products with *aa* selectivity reaches up to 96.2%. This result suggest, Ag nanoparticles directly influencing the performance of WOx nanoclusters supported on CNx. The small size silver nanoparticles itself is not highly active but it stimulated oxidation behavior of the WOx nanoclusters for selective production of adipic acid. We consider that the synergy between Ag and WO_3 nanostructure are crucial to enhance the catalytic activity of the AgWCNx materials towards the *aa* yield. Where the combined synergistic effect of Ag and WO_3 nanoclusters supported on CNx matrix is the primary important factor for complete oxidation for *aa* formation.

As a reference we have also studied the catalysis of AgWCNx synthesized through the wet impregnation method. The AgWCNx-2^{imp} possesses similar activity with WCNx (Table 2, entry 11). Commercially available Ag NPs and WOx nanoparticles employed for cyclohexene oxidation also gives negligible results (not shown). It appears molecular lever dispersion of Ag and WO_3 (experienced from TEM and e mapping) are the driving factor for the oxidation product beyond cyclohexenol, cyclohexenone and cyclohexane oxide.

Effect of different reaction parameter

The effect of temperature on cyclohexene conversion and adipic acid selectivity is shown in Figure 6a. AgWCNx-2 gives the maximum yield of *aa* at 90°C under atmospheric pressure. Further increasing in the temperature above 90°C decrease the yield of adipic acid which might be due to the rapid decomposition of H_2O_2. Whereas, temperature below 90°C also decrease the yield of adipic acid and enhances production of cyclohexanol and cyclohexanone. Periodic increase in cyclohexene oxidation as a function of reaction time was noticed and shown in Figure 6b; indicates the increasing activity with time. From the graph it can be seen, that with start of reaction (after 2h) cyclohexene oxide is formed as the major product along with cyclohexenol and cyclohexenone (form directly from cyclohexene, Scheme-1). After 6h, cyclohexane oxide completely oxidize to intermediate oxidation product like cyclohexanediol, cyclohexanedione. Adipic acid formation 1st noticed after 10h, along with oxepane-2,7-dione, oxepane-2,7-diol. A steady formation of adipic acid was noticed till 16th h and cyclohexene conversion reaches maximum 90.2% with 75.1% selectivity of adipic acid. At 18h time on stream maximum conversion of cyclohexene (92.2%) and selectivity (96.2%) is observed.

The effect of H_2O_2 was also evaluated as a function of cyclohexane conversion and *aa* selectivity (Figure 6c). It was observed, the *aa* yield gradually increase with the increase in H_2O_2 added. Although, used of excess oxidant dot not causes

complete oxidation, which may me because of the saturation in H_2O_2 is decomposed over catalytic surface spontaneously.[29] It is been experienced that 4.5 ml of H_2O_2 is sufficient for optimum *aa* yield (Figure 6c). While increasing the amount of H_2O_2 (5 ml) do not affect the adipic acid yield; which might be due to the release of excess H_2O which will suppress the substrate adsorption on catalytic surface. Figure 6d shows the effect of Ag:W ration as a function of cyclohexene conversion and *aa* selectivity. As it discussed above, that AgCNx have better oxidation capability than WCNx; which reflects on the result plotted in Figure 6d. Adipic acid formation was noticeable with AgWCNx, which was tripped to 84.1% (*aa* selectivity) with 0.25:2.5 ratio of Ag to WO_3. This result indicate remarkable increase in adipic acid selectivity and cyclohexene activity with the combination of Ag and WO_3 over mesoporous CNx.

Role of Ag and peroxo-tungsten complex

From the previous report we experienced that tungsten can exist in number of oxidation state It is supposed that the reaction of H_2O_2 with catalyst formation of peroxo tungsten species which is electrophilic in nature. While the vacant orbitals in unsaturated alkenes are interacted towards Ag (1) metal d^{10} electronic shells. So homogeneously distributed silver nanoparticles activate alkenes that can enhance its rate of oxygen transfer from peroxo tungsten complex. Moreover CNx supports can enhance rate of hydrolysis step.

In order to justify the formation of peroxo-tungsten species we have withdrawn catalyst in between reaction and dried under vacuum at low temperature and subjected to Raman spectroscopy (Figure S11, supporting information). We observed a new adsorption peak at 574 and 873 cm^{-1} for the WCNx catalyst with corresponds to $v(W(O_2))_{asymp}$ and v(O–O) Raman band of peroxo-tungsten species.[30] The intensity of the new Raman bands increased with the addition of Ag (i.e. AgWCNx catalyst), which demonstrate increase of peroxo-tungsten species. Thus it can be conclude that with the addition of Ag to WO_3 the formation of peroxo tungsten species increases and as a result the possibility of total oxidation of cyclohexene increases.

Inter-relation between acidity and activity

An attempt to inter-relate the surface acidity with the catalytic activity we plotted the surface acidity and activity data vs different AgWCNx catalyst and the results is shown in Figure S10a. The data suggest that increase in the number of acid sites enhances the cyclohexane conversion and appropriate loading and acidity gives the best yield of *aa*. Furthermore, the structure calculated from DFT of different catalysts, we get the idea how acidity and activity are related. In TS-1 for AgWCNx-1 (Ag: W is 0.25:1.25) Figure S10b, we observe that one oxygen atom from WO_3 makes bond with Ag atom of silver nanoparticle. Due to high electro negativity of oxygen, addition of oxygen to silver nanoparticle makes it electro positive which helps to Ag-O-Ag bond formation (in Figure S10b) and peroxide decomposition to yield cyclohexanol in the initially stage of reaction. Thereby, it is obvious that increase in the amount of WO_3 (in case of AgWCNx-2, 3) helps to form more and more W-O-Ag bonds with the silver nanoparticles which make it more electro positive and facilitates cyclohexanol formation, which further oxidized to form *aa*. Thus, we observe increase of activity with the increase of acidity.

Reaction mechanism

From the above reaction data we have concluded a mechanism which is shown in Scheme 1. Cyclohexene oxidation in presence of H_2O_2 is a four step process namely, 1) epoxidation, 2) hydrolysis 3) alcohol oxidation and 4) Baeyer-Villiger rearrangement. We experience oxidation via allylic oxidation and epoxidation routes in the beginning hours of the reaction as experienced Cao *et al*. over nitrogen doped carbon nanotubes.[31] As a result we sported cyclohexenol, cyclohexanone along with cyclohexane oxide (major); after 6^{th} h of reaction cyclohexane oxide completely disappeared to form higher oxidation product (Figure 6b) via hydrolysis. Intermediate compound like cyclohexanediol and cyclohexanedione thus formed, undergo Baeyer-Villiger rearrangement to form oxepane-2,7-diol. W is well known catalyst for BV- rearrangement in presence of a Lewis acids or H_2O_2 in combination of Ag.[32] Further oxidation of oxepane-2,7-diol forms oxepane-2,7-dione, which appears maximum after 10^{th} h of reaction. Finally, hydrolysis of oxepane-2,7-dione forms adipic acid. Although we observed the formation of *aa* at 10^{th} h of the reaction but it took 18 h to maximize the yield of aa (88.6) and complete oxidation of the intermediate compound shown in Scheme 1.

Mechanistic studies

We studied energy profile for this path for three different catalysts; a) AgCNx, b) WCNx and c) AgWCNx. Gaussian 09 [33] package is used for all density functional based (DFT)[34] calculations. We used B3LYP functional[35] and LanL2DZ basis[36]. Energy profile diagrams are presented in Figure7a-c.

We observed that when AgCNx and WCNx are used as catalyst, reaction go through epoxide formation. Activation energy for this state for AgCNx catalyst (29.58 kcal/mol) is higher than that of WCNx catalyst (24.86 kcal/mol). But, for other two oxidized products activation energies are higher for WCNx which is correlated with our experimental observations (Table2 entry 3-4). From this study we may conclude that WCNx is better catalyst for epoxidation but AgCNx is better catalyst for overall oxidation process. Activation energies for TS-4 are very high for both catalysts (136.55 and 126.01 kcal/mol respectively) and have effective positive values (32.40 and 21.86 kcal/mol respectively). Thus, we get only cyclohexanol, cyclohexanone and cyclohexane oxide as major product when AgCNx and WCNx are used separately. For AgCNx we get trace amount of adipic acid (0.9% only) as activation energy of TS-6 (113 kcal/mol) is less than that for WCNx catalyst (188.25 kcal/mol). But when Ag nanoparticle is embedded on WCNx (AgWCNx) and used as catalyst we get very good yield of adipic acid.

When AgWCNx is used as catalyst, reaction goes through a different mechanism. Instead of epoxide formation at initial stage, cyclohexanol is formed. Cyclohexanol is a more stable product than epoxide. Free energy change for epoxide formation is -33.73 kcal/mol where for cyclohexanol formation free energy change is -76.57 kcal/mol. Probably, activation energy for this process without AgWCNx catalyst is very high enough such that we get only epoxide product at step-1 when AgCNx and WCNx are used separately. We are unable to get proper transition state to form cyclohexanol as initial product when AgCNx and WCNx are used separately. But, when Ag-WCNx is used, activation energy for cyclohexanol formation is only 7.67 kcal/mol. Due to more change in free energy (- 42.84 kcal.mol) at initial stage and reduction of

10.1002/chem.201703111

activation energies in different intermediate states, there is no real energy barrier (i.e. effective energy barrier) to form adipic acid when AgWCNx is used as catalyst. Thus, we get very good yield of adipic acid. Other than that, reaction is highly selective for this catalyst.

Role of Catalyst

To understand why AgWCNx is more active than individual catalysts (AgCNx and WCNx) we compare HOMO of TS-1 for these catalysts which are presented in Figure 8a-c. We observed that when AgCNx or WCNx is used there is no orbital overlap between catalyst and reactant. Thus, oxygen transfer is not easy and hence activation energy is high. On the other hand when AgWCNx is used HOMO electron cloud partially distributed over peroxide and cyclohexane radical. Thus oxygen transfer become easier and hence activation energy is less.

Recycle and reusability testing

To investigate the catalyst leaching into the reaction medium, Sheldon's hot filtration test was performed.[37] Filtration of the catalyst was done at hot condition followed by continuation of reaction in absence of catalyst. After the filtration, the filtrate was added to the vessel again and the reaction was continued for another 10 h. No increase in substrate conversion was observed. This observation confirms the absence of any effective leaching of any active species in reaction medium. Moreover, no trace of either tungsten or silver has been found in ICP analysis of the hot filtrate portion.

To check the reusability of the catalyst we have filtered and dried the catalyst at the end of the reaction. Prior to start consecutive run the catalyst was activated again in N_2 atmosphere for several hours at 350°C. The result of the successive run (Figure S12) shows drop of cyclohexene conversion although the *aa* selectivity changed marginally. The drop in cyclohexene is caused due to the catalyst loss during handling, in order to prove it we have calculated the TOF (turn-over-frequency, in h^{-1}) in respect to conversion of cyclohexene. The result (in Figure S12) shows no effective change in TOF values, which proves the catalyst a novel water resistance reusable catalyst for further use.

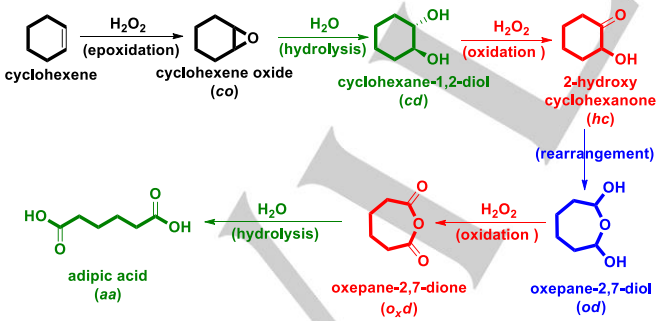

Scheme 1. Mechanistic pathways of cyclohexene oxidation to *aa* with H_2O_2. (colour coding represents different kind of reaction undertaken during the process)

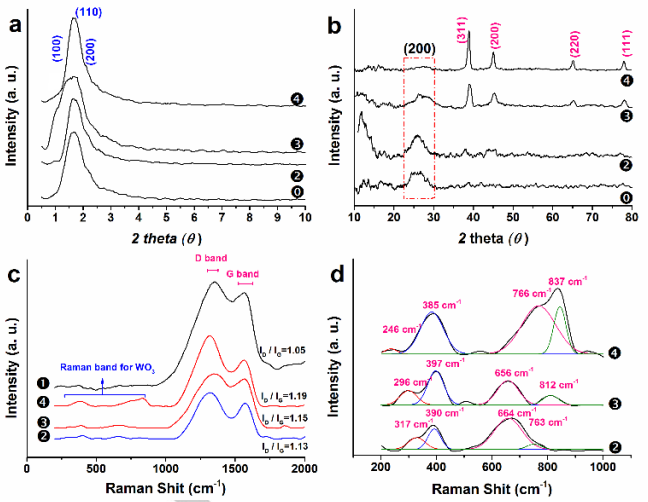

Figure 1. (a) Low angle and (b) high angle X-ray diffraction pattern; (c) Raman spectra of graphitic carbon and (d) W of ❶ CNx; ❶WCNx; ❷ AgWCNx-1; ❸ AgWCNx-2 and❹ AgWCNx-3.

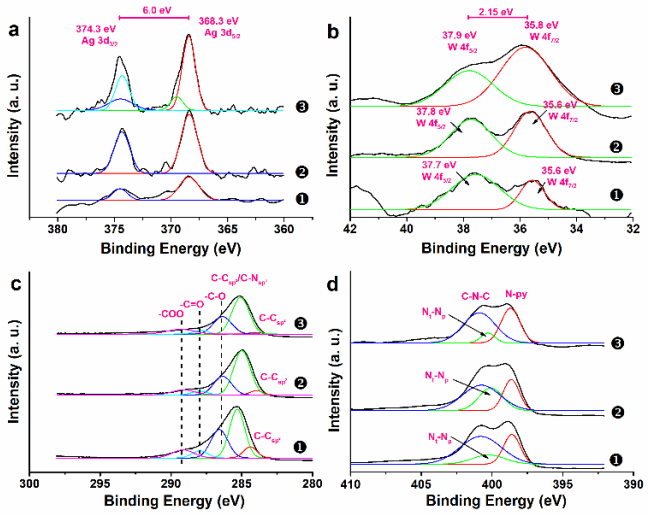

Figure 2. XP spectra of (a) Ag 3d, (b) W 4f, (c) C 1s and (d) N 1s of bimetallic CNx catalyst. Note:❶ AgWCNx-1,❷ AgWCNx-2 and ❸ AgWCNx-3.

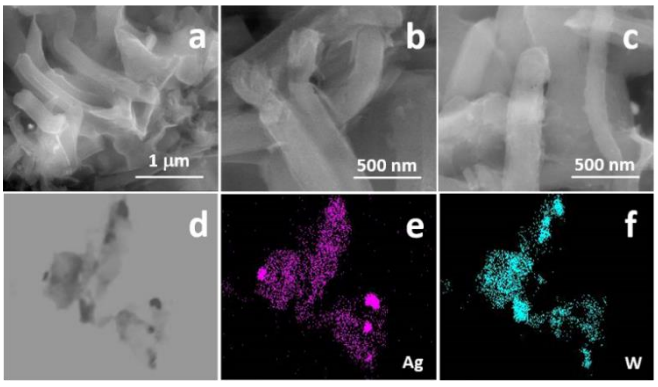

Figure 3. FESEM images of AgWCNx-2 catalyst showing wheatlike fibres (a-c); corresponding image (d) used for e-mapping for Ag (e) and W (f) respectively.

10.1002/chem.201703111

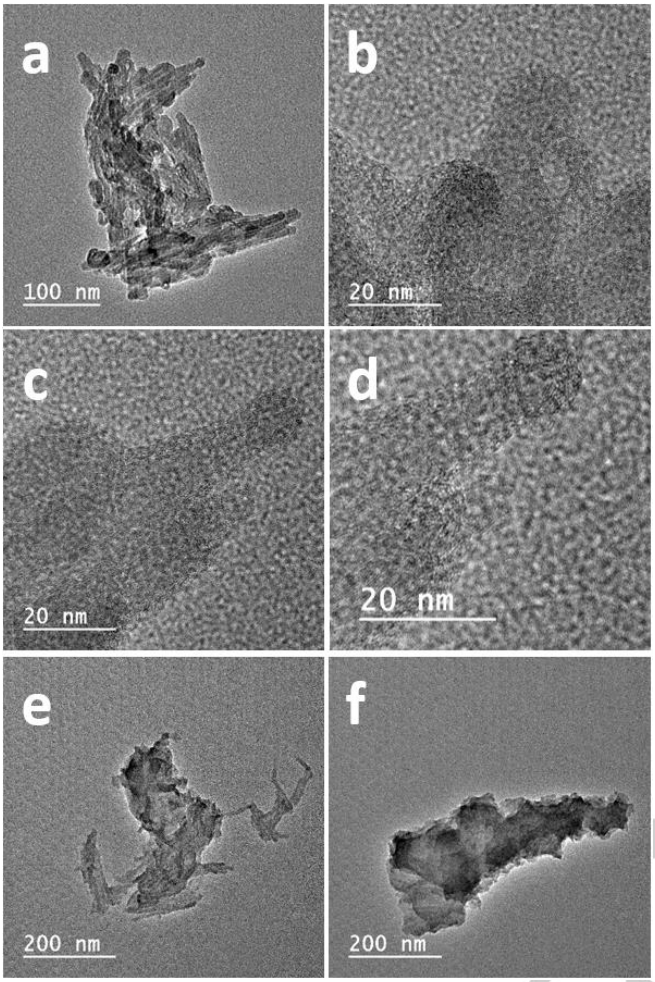

Figure 4. High resolution TEM of supported CNx catalyst, (a-d) HR-TEM images of AgWCNx-2 in different magnification; (e) AgWCNx-1 and (f) AgWCNx-3 catalyst.

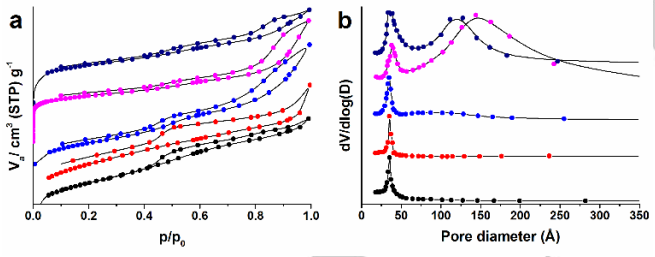

Figure 5. (a) N_2 adsorption desorption isotherm and (b) BJH plot of (●)WCNx; (●)AgWCNx-1; (●) AgWCNx-2 (●) AgWCNx-3 and (●) AgCNx respectively.

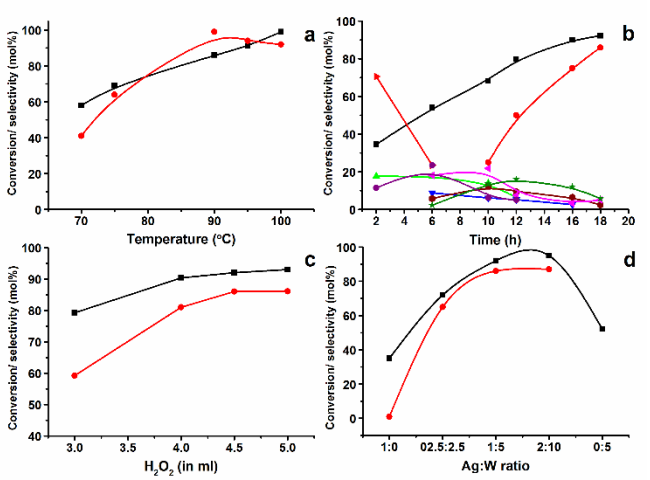

Figure 6. Cyclohexene conversion and product selectivity as a function of (a) temperature, (b) time, (c) amount of oxidant added and (d) Ag to W ration in the working catalyst.
Representation: (■) cyclohexene conversion, selectivity to (●) adipic acid, (▶)cyclohexene oxide, (●) cyclohexanol, (▲) cyclohexanone (▼) cyclohexanediol, (⬢) cyclohexanedione, (◀) oxepane-2,7-dione, (★) oxepane-2,7-diol.

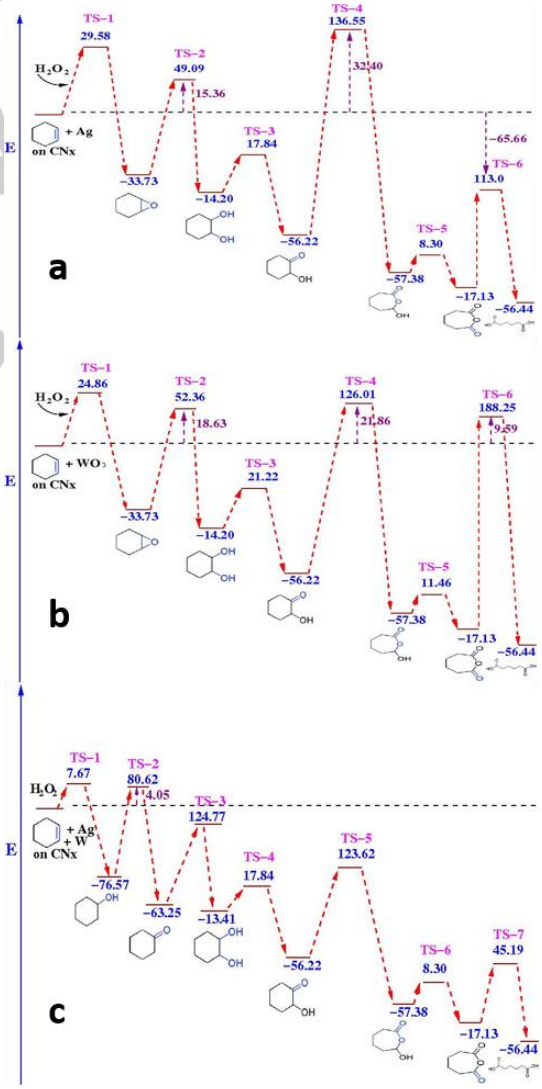

Figure 7. Energy profile diagram (a) for AgCNx, (b) for WCNx and (c) for AgWCNx. Energies are in kcal/mol unit.

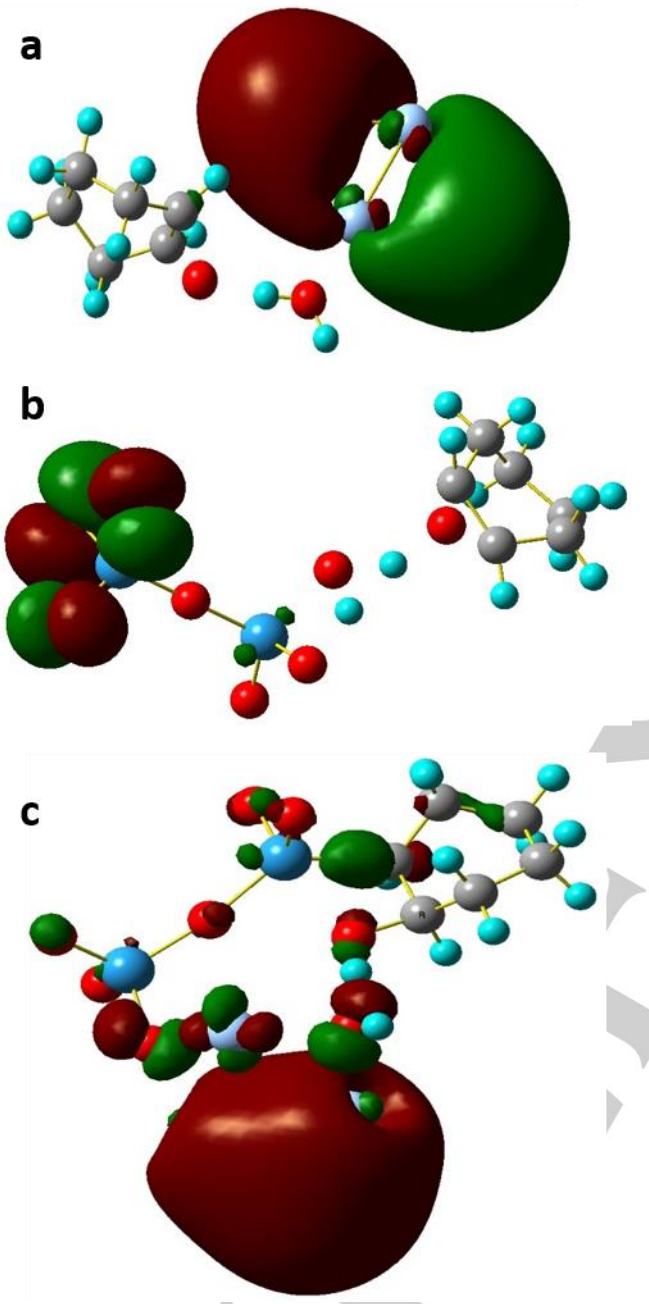

Figure 8. HOMO of TS-1 for different catalyst. (a) AgCNx, (b) WCNx and (c) AgWCNx

Table 1. Physiochemical properties of Ag-W/CNx catalyst.

Catalyst	Surface Area[a]	Pore Volume[b]	Pore diameter[c]	Acidity[d]	ICP data (%) Ag	W	N [wt %][e]
CNx	359	0.34	3.84	-	-	-	-
Ag/W-SiO_2	467	0.38	3.32	NA	0.52	2.92	-
AgWCNx-1	349	0.43	5.01	80.2	0.22	1.14	13.50
AgWCNx-2	328	0.34	4.05	108	0.50	2.80	13.39
AgWCNx-3	313	0.28	3.65	120	0.93	4.41	13.07

a BET surface area in m^2/g; b BJH pore volume in cm^2/g. c BJH pore diameter in nm; d NH_3-TPD results: amount of NH_3 adsorbed in µmol NH_3 g^{-1}; [e] determined by CHNS analyser

Table 2. Experimental data for the direct oxidation of cyclohexene to adipic acid.

Sl No	Catalyst	X_c	Selectivity co	ol-one	hc	od	oxd	*aa*	ui	TOF[a] ($\times 10^2$)
1	bare	~4	41.3	58.1	0.6	-	-	-	-	-
2	CNx	~5	41.7	47.0	11.3	-	-	-	-	-
3	WCNx	65.7	73.1	9.5	12.1	5.4	-	-	-	-
4	AgCNx	25.1	40.0	27.5	25.3	5.1	1.2	0.9		0.51
5	$WCNx^{pmix}$	39.4	89.2	5.1	5.7	-	-	-	-	-
6	$AgCNx^{pmix}$	13.9	46.9	31.3	19.7	2.1	-	-	-	-
7	AgW-SiO_2	71.5	69.8	10.6	13.5	6.1	-	-	-	-
8	AgWCNx-1	89.9	-	-	-	5.2	8.7	84.1	1.0	73.5
9	AgWCNx-2	92.2	-	-	-	-	-	96.2	3.8	35.0
10	AgWCNx-3	≥99.9	-	-	-	-	-	95.0	5.0	23.7
11	$AgWCNx\text{-}2^{imp}$	68.5	24.5	14.4	32.6	8.2	3.5	9.7	1.1	2.11

Condition: 12 mmol (or 1 g) cyclohexene; 10 ml methanol; 0.05 g catalyst; 90°C temperature; 18 h of reaction [a] after 4 consecutive regeneration (treated with 5%H_2 with balance He at 250°C for 1 h). [a] TOF (x 10^2) was calculate on the basis of aa yield.
Abbreviation used: co = cyclohexene oxide; ol-one = cyclohexenol and cyclohexenone; hc = 2-hydroxy cyclohexanone; od = oxepane-2,7-diol; oxd = oxepane-2,7-dione; aa = adipic acid ; ui = unidentified products. Note: The water formation is not taken into account for conversion as well as selectivity calculation.

Conclusions

In conclusion, we have demonstrate an efficient approach for the preparation of silver grafted on mesoporous WCNx. The material account high specific surface area of 328 m^2/g with coexistence of micro and mesopore. HR-TEM shows 0.2-0.3 nm 2D channels, which is consist with mesopores of 3 to 4 nm within the material. A transfer of electron density from WO_3 to silver atoms also has been notices. The catalyst found highly selective for the one-port production of adipic acid from cyclohexene. It has been observed that AgWCNx catalysts were efficient for the direct conversion of adipic acid in respect to their monometallic counters. DFT calculation shows no orbital overlap between the catalyst (monometallic catalysts) and reactant, which results restricted oxygen transfer and high activation energy compared to AgWCNx catalyst. The results indicate that the AgWCNx-2 catalyst gives

the best results with 92.2% of cyclohexene conversion and 96.2% adipic acid selectivity.
The present catalyst is easy to recycled, and reused; ICP analysis shows no accountable leaching of active metals. Such one-step method using H_2O_2 makes this oxidation process highly efficient and eco-friendly compared to the current industrial two-step oxidation process. Furthermore, the new mesoporous CNx based catalyst provides a novel water resistance catalyst system for highly selective single-step synthesis of adipic acid.

Experimental Section

Material preparation

AgWCNx has been prepared in two steps. In the 1st step Ag/WOx embedded silica template was prepared, followed by nano-casting of carbon and nitrogen precursor on template to prepare AgWCNx nanocomposite. The materials with three different metal content (Ag: W= 1:1, 1:3, 1:5) were synthesized.

Synthesis of template: Ag-WOx-SiO_2

Ag/WOx embedded silica template was prepared by modifying the synthesis strategy detailed in our previous paper.[2, 38] Firstly, 2g of triblock copolymer P123 was dissolved in 40 ml water. Upon complete dissolution, 0.5 M sodium tungstate solution (1, 2.5, and 5 ml) was added to it. Acidity of the solution was maintained with introducing 60ml 2M HCl solution. The above mixture was kept under continuous stirring at 35°C for aging. Before adding silver ion precursors 0.1 ml aniline was mixed to the above solution. After adding 0.5 M silver nitrate (0.5, 1,2ml) solution 4.5 g of tetraethyl orthosilicate (TEOS), as silica source was added dropwise to above mixture and kept under continuous stirring at constant temperature. After a day, the obtained solution was hydrothermally treated at 100°C for 48h. To get the Ag-WOx-SiO_2, the obtained gel was allowed to cool, filter and washed with 50 ml ethanol water mixture (1:4) and finally calcined at 550°C for 6h.

Material synthesis: AgWCNx

0.5 g of above synthesized Ag-WOx-SiO_2 was mixed with 2.2g ethylene diamine and 6g CCl_4 in round bottom flask. To polymerize above mixture was placed on reflux at 90°C for 6h. After that carbonization of above materials was carried out under nitrogen atmosphere at 600°C for 6-8h. To remove silica template we have treated the above material with 1M NaOH solution for 3-4h at 100°C. Finally, it was filter, washed with 3-4 liter water (until pH-7) and dried. For complete removal of silica the similar process was repeated 2-3 times. The outcome material was coded as AgWCNx-1, 2 and 3; where 1, 2 and 3 represents the Ag: W ratio= 0.25:1.25, 0.5:2.5, 1:5.

Catalyst Characterization

Detailed morphology of the supported CNx catalysts were analyzed using field emission scanning electron microscopy (FE-SEM) (FEI Quanta 200 F). The same instrument was used for the energy dispersive X-ray spectroscopy (SEM-EDS). A JEM-2010DM (JEOL, Japan) was used to obtain the high resolution-transmission electron microscopic images of different Cnx catalyst. The BET surface area & pore network of the mesoporous nitrogen rich CNx materials were characterized by N_2 adsorption-desorption isotherm at 196°C using an Autosorb 1C setup (Quantachrome). Prior to the experiments, samples were degassed under 1×10^{-5} Torr vacuum for 2 h at 200°C and the BET specific surface areas were calculated from the adsorption data within the relative pressure (P/P_o) range of 0.06 to 0.2. The pore size distributions were calculated using the Barrett-Joyner-Halenda (BJH) analysis and the maximum distribution of pore size was considered to be the average pore size. The pore volume was considered as the volume of liquid nitrogen adsorbed at P/P_o = ca. 1. Low angle X-ray diffraction pattern (XRD) were acquired with a Bruker-AXS, D8-Advance diffractometer. Cu-Kα were used as the source of radiation and all the data was collected in θ–2θ geometry with a position sensitive detector. Wide angle XRD diffraction patterns were acquired in 2θ range of 10-80° with an analytical MPD diffractometer and a Cu-Kα radiation source (λ=1.5418 Å) ware used at an operating voltage of 45 kV. Raman spectrum of the supported CNx catalyst was collected using a HORIBA XploRA micro-Raman spectroscopy instrument, HORIBA Ltd., Japan. 532 nm semiconductor laser was used as the incident light for all of the experiments.

The surface analysis of all the catalysts was carried out by a K-Alpha (Thermo Scientific Corp.) X-ray photoelectron spectrometer. Measurements were carried out under ultra-high vacuum (UHV) set-up armed with an Al Kα monochromatic X-ray source (hv = 1486.6 eV), operated at 14.5 kV. The chamber pressure was maintained at 7×10^{-10} mbar thought the experiment. All the binding energy (BE) were normalized using sp2 hybridized C 1s line at BE, 284.5 eV. The Casa XPS program [39] with a 70:30 Gaussian-Lorentzian function and Shirley background subtraction was used for deconvolution of XPS-peak. H_2-TPR of the NG-CNx catalyst was carried out in a Micromeritics, Auto Chem II 2920 instrument. Prior to each experiment, the catalysts was heated at 650°C for 2 h in He and then placed in 10% H_2/Ar with a flow rate of 40 mL min^{-1} in the temperature range of 40-800 °C with an increment of 10°C/min. NH_3-TPD of the supported CNx materials was also carried out in the same instrument, where the consumed NH_3 was estimated by a thermal conductivity detector (TCD). Approximately 0.025 g sample was taken with a gas flow rate of 16 mL/min and the heating rate of 10 °C/min.

Catalyst Testing

The liquid phase cyclohexene oxidation was carried out in a 50ml double necked round bottom flask. Typically 50mg of the catalyst with 1g cyclohexene, and hydrogen peroxide (30% aqueous solution) 3-5 ml and 10ml methanol as a solvent was added into it with a magnetic bar. The flask was then placed in preheated oil bath. The hydrogen peroxide was added dropwise up-to 30 minutes. The little aliquot of the sample mixture was collected at regular interval for analysis. The reaction products were analyzed using an Agilent 7890A, gas chromatography equipped with a MXT-WAX (30m x 0.28nm, 0.25 µm film thickness) capillary

column and a FID detector. The activity of the catalyst was calculated as:

$$Conversion\ (mole\%) = \frac{Moles\ of\ reactant\ reacted\ (mole\%)}{Moles\ of\ reactent\ initially\ used\ (mole\%)} \times 100$$

$$Selectivity\ (mole\%) = \frac{Moles\ of\ product\ (mole\%)}{Moles\ of\ reactant\ reacted\ (mole\%)} \times 100$$

Recycle and reusability testing

To investigate whether any active species of the catalyst were leaching into the reaction medium, we carried out the reaction under selected conditions with Ag/WOx-CNx catalyst. The reaction was stopped after 3 h, the catalyst was separated by hot filtration and conversion of substrate was estimated. The filtrate was added to the vessel again, and the reaction was continued for another 10 h. No increase in substrate conversion was observed; it remained the tungsten species of the catalyst into the reaction mixture; the catalyst truly acted as if it were heterogeneous. This observation confirms the complete absence of leaching of any active species in reaction medium. Moreover, no trace of tungsten has been found in ICP analysis of the hot filtrate portion.

Acknowledgements

We are grateful to DST, New Delhi for the financial support in terms of Fast track young scientist grant. Reena Goyal and Nikita Singhal acknowledges Council for Scientific and Industrial Research (CSIR), India. All the authors express gratitude to Analytical Science Division, CSIR-Indian Institute of Petroleum for the analytical support.

Keywords: carbon nitride • adipic acid • oxidation • green chemistry • silver tungsten

[1] R. Goyal, B. Sarkar, A. Bag, N. Siddiqui, D. Dumbre, N. Lucas, S. K. Bhargava, A. Bordoloi, *J. Catal.* **2016**, *340*, 248-260.
[2] R. Goyal, B. Sarkar, N. Lucus, A. Bordoloi, *ChemCatChem* **2014**, *6*, 3091-3095.
[3] S. Ghosh, S. S. Acharyya, S. Adak, L. N. S. Konathala, T. Sasaki, R. Bal, *Green Chem.* **2014**, *16*, 2826-2834.
[4] R. Mayer, *Greenwood Press, London* **2007**.
[5] (a) Y. Wen, X. Wang, H. Wei, B. Li, P. Jin, L. Li, *Green Chem.* **2012**, *14*, 2868-2875; (b) K. Sato, M. Aoki, R. Noyori, *Science* **1998**, *281*, 1646-1647.
[6] (a) C. Venturello, M. Ricci, *The Journal of Organic Chemistry* **1986**, *51*, 1599-1602; (b) Y. Ishii, K. Yamawaki, T. Ura, H. Yamada, T. Yoshida, M. Ogawa, *The Journal of Organic Chemistry* **1988**, *53*, 3587-3593.
[7] (a) Z. Bohström, I. Rico-Lattes, K. Holmberg, *Green Chem.* **2010**, *12*, 1861-1869; (b) M. Vafaeezadeh, M. M. Hashemi, *Rsc Advances* **2015**, *5*, 31298-31302; (c) L. Wang, M. Huang, Z. Chen, Z. Yang, M. Qiu, K. Wang, W. Zhang, *CrystEngComm* **2016**, *18*, 8688-8695.
[8] (a) W. Wang, H. Liu, G. Ding, P. Zhang, T. Wu, T. Jiang, B. Han, *ChemCatChem* **2012**, *4*, 1836-1843; (b) F. Schwab, M. Lucas, P. Claus, *Angew. Chem. Int. Ed.* **2011**, *50*, 10453-10456; (c) H. Liu, T. Jiang, B. Han, S. Liang, W. Wang, T. Wu, G. Yang, *Green Chem.* **2011**, *13*, 1106-1109.
[9] (a) M. Jin, Z.-M. Cheng, *Catal. Lett.* **2009**, *131*, 266-278; (b) F. Patcas, F. Patcas, *Catal. Today* **2006**, *117*, 253-258; (c) H. Zhu, Q. Ge, W. Li, X. Liu, H. Xu, *Catal. Lett.* **2005**, *105*, 29-33.
[10] Y. Deng, Z. Ma, K. Wang, J. Chen, *Green Chem.* **1999**, *1*, 275-276.
[11] M. Vafaeezadeh, M. M. Hashemi, M. Shakourian-Fard, *Catal. Commun.* **2012**, *26*, 54-57.
[12] H. Li, W. Zhu, X. He, Q. Zhang, J. Pan, Y. Yan, *React. Kinet. Catal. Lett.* **2007**, *92*, 319-327.
[13] K. Fujitani, T. Mizutani, T. Oida, T. Kawase, *Journal of oleo science* **2009**, *58*, 37-42.
[14] P. Jin, Z. Zhao, Z. Dai, D. Wei, M. Tang, X. Wang, *Catal. Today* **2011**, *175*, 619-624.
[15] S. O. Lee, R. Raja, K. D. Harris, J. M. Thomas, B. F. Johnson, G. Sankar, *Angew. Chem.* **2003**, *115*, 1558-1561.
[16] (a) G. Lapisardi, F. Chiker, F. Launay, J. Nogier, J. Bonardet, *Microporous Mesoporous Mater.* **2005**, *78*, 289-295; (b) G. Lapisardi, F. Chiker, F. Launay, J.-P. Nogier, J.-L. Bonardet, *Catal. Commun.* **2004**, *5*, 277-281.
[17] R. Noyori, M. Aoki, K. Sato, *Chem. Commun.* **2003**, 1977-1986.
[18] R. Goyal, D. Dumbre, L. N. S. Konathala, M. Pandey, A. Bordoloi, *Catal. Sci. Tech.* **2015**, *5*, 3632-3638.
[19] (a) B. Sarkar, C. Pendem, L. N. Sivakumar Konathala, R. Tiwari, T. Sasaki, R. Bal, *Chem. Commun.* **2014**, *50*, 9707-9710; (b) B. Sarkar, P. Prajapati, R. Tiwari, R. Tiwari, S. Ghosh, S. Shubhra Acharyya, C. Pendem, R. Kumar Singha, L. N. Sivakumar Konathala, J. Kumar, T. Sasaki, R. Bal, *Green Chem.* **2012**, *14*, 2600-2606.
[20] S. Zhang, H. Li, Q. Zhong, *Appl. Catal., A* **2012**, *435*, 156-162.
[21] A. A. Taha, F. Li, *Catal. Sci. Tech.* **2014**, *4*, 3601-3605.
[22] L. Xu, M.-L. Yin, S. F. Liu, *Scientific reports* **2014**, *4*.
[23] X. An, C. Y. Jimmy, Y. Wang, Y. Hu, X. Yu, G. Zhang, *J. Mater. Chem.* **2012**, *22*, 8525-8531.
[24] B. Sarkar, B. Chelliahn, P. V. Rao, G. Sriganesh, N. V. Choudary, R. Ravishankar, *Advanced Porous Materials* **2015**, *3*, 63-68.
[25] C. Bittencourt, M. P. Felicissimo, A. Felten, L. A. O. Nunes, P. Ivanov, E. Llobet, J. J. Pireaux, L. Houssiau, *Appl. Surf. Sci.* **2005**, *250*, 21-28.
[26] B. Sarkar, R. Goyal, C. Pendem, T. Sasaki, R. Bal, *J. Mol. Catal. A: Chem.* **2016**, *424*, 17-26.
[27] M. D. Soriano, P. Concepcion, J. M. L. Nieto, F. Cavani, S. Guidetti, C. Trevisanut, *Green Chem.* **2011**, *13*, 2954-2962.
[28] S. Van de Vyver, Y. Roman-Leshkov, *Catal. Sci. Tech.* **2013**, *3*, 1465-1479.
[29] K. R. Naqvi, J. Marsh, V. Chechik, *Dalton Transactions* **2014**, *43*, 4745-4751.
[30] K. Kamata, K. Yonehara, Y. Sumida, K. Hirata, S. Nojima, N. Mizuno, *Angew. Chem. Int. Ed.* **2011**, *50*, 12062-12066.
[31] Y. Cao, H. Yu, F. Peng, H. Wang, *ACS Catalysis* **2014**, *4*, 1617-1625.
[32] S. Ghosh, S. S. Acharyya, R. Singh, P. Gupta, R. Bal, *Catal. Commun.* **2015**, *72*, 33-37.
[33] M. Frisch, G. Trucks, H. B. Schlegel, G. Scuseria, M. Robb, J. Cheeseman, G. Scalmani, V. Barone, B. Mennucci, G. Petersson, *Inc., Wallingford, CT* **2009**, *200*.
[34] P. Hohenberg, W. Kohn, *Phys. Rev.* **1964**, *136*, B864-B871.
[35] (a) A. D. Becke, *Phys. Rev. A* **1988**, *38*, 3098-3100; (b) C. Lee, W. Yang, R. G. Parr, *Phys. Rev. B* **1988**, *37*, 785-789.
[36] L. E. Roy, P. J. Hay, R. L. Martin, *J. Chem. Theory Comput.* **2008**, *4*, 1029-1031.
[37] H. Lempers, R. Sheldon, *J. Catal.* **1998**, *175*, 62-69.
[38] R. Goyal, B. Sarkar, A. Bag, F. Lefebvre, S. Sameer, C. Pendem, A. Bordoloi, *J. Mater. Chem. A* **2016**, *4*, 18559-18569.
[39] N. Fairley, *Casa Software Ltd* **2009**.

10.1002/chem.201703111

WILEY-VCH

Entry for the Table of Contents (Please choose one layout)

Layout 1:

FULL PAPER

Adipic acid in a pinch: Direct conversion of cyclohexene into *aa* is carried out in the presence of silver grafted mesoporous W-CNx catalyst. High activity and yield is achieved and the catalyst can be successfully recycled in consecutive runs. Detailed surface study and time dependent product formation is monitored to postulated the most possible reaction mechanism.

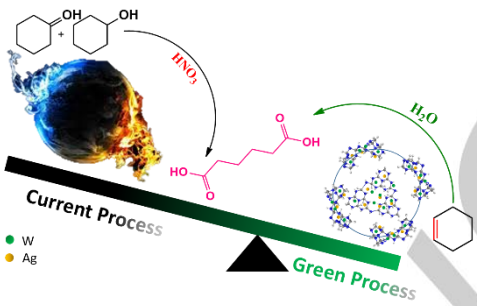

*Reena Goyal, Siddharth Sameer, Dr. Bipul Sarkar, Dr. Arijit Bag, Nikita Singhal, and Dr. Ankur Bordoloi**

Page No. – Page No.

Synthesis of AgWCNx nanocomposite for one-step conversion of Cyclohexene to Adipic Acid and its mechanistic studies